

## Polyaniline Nanofibers: Facile Synthesis and Chemical Sensors

Jiaxing Huang,<sup>†</sup> Shabnam Virji,<sup>†,‡</sup> Bruce H. Weiller,<sup>\*,‡</sup> and Richard B. Kaner<sup>\*,†</sup>

Department of Chemistry and Biochemistry, Exotic Materials Institute and California NanoSystems Institute,  
University of California, Los Angeles, Los Angeles, California 90095-1569, Materials Processing and Evaluation  
Department, Space Materials Laboratory, The Aerospace Corporation, P.O. Box 92957/M2-248,  
Los Angeles, California 90009

Received September 2, 2002; E-mail: (R.B.K.) kaner@chem.ucla.edu, (B.H.W.) bruce.h.weiller@aero.org

Polyaniline is a conducting polymer that has been widely studied for electronic and optical applications.<sup>1</sup> Unlike other conjugated polymers, polyaniline has a simple and reversible acid/base doping/dedoping chemistry enabling control over properties such as free-volume<sup>2</sup>, solubility<sup>3</sup>, electrical conductivity,<sup>4</sup> and optical activity.<sup>5,6</sup> In recent years, one-dimensional (1-D) polyaniline nanostructures, including nanowires, rods, and tubes have been studied with the expectation that such materials will possess the advantages of both low-dimensional systems and organic conductors.

Syntheses of polyaniline 1-D nanostructures have been carried out both chemically and electrochemically by polymerizing the monomer with the aid of either a "hard" or a "soft" template. Examples of hard templates include zeolite channels,<sup>7</sup> track-etched polycarbonate<sup>8,9</sup> and anodized alumina.<sup>8,10</sup> Soft templates, such as surfactants,<sup>11</sup> micelles,<sup>12–14</sup> liquid crystals,<sup>15</sup> thiolated cyclodextrins,<sup>16</sup> and polyacids,<sup>17</sup> are reported to be capable of directing the growth of polyaniline 1-D nanostructures with diameters smaller than 100 nm. Physical methods, including electrospinning<sup>18,19</sup> and mechanical stretching,<sup>20</sup> have also been used to make polyaniline nanofibers. In earlier work, polyaniline fibrils of ~100 nm in diameter, with a compact microspheruloid underlayer,<sup>21</sup> were found on the surface of electrochemically polymerized films. Interconnected network-like structures with polyaniline "nano-linkers" 10–50 nm wide have also been identified in polymer blends.<sup>22</sup>

Despite the variety of current synthetic approaches to polyaniline nanostructures, there is a need for a practical synthetic method capable of making pure, uniform, and template-free polyaniline nanostructures with small diameters (sub-100 nm) in bulk quantities. Such a synthetic method should prove useful for properties dependent on ultra-small, low-dimensional structures, such as sensors.

Here we report a facile chemical route to high-quality polyaniline nanofibers under ambient conditions using aqueous/organic interfacial polymerization. The nanofibers have nearly uniform diameters between 30 and 50 nm with lengths varying from 500 nm to several micrometers. Gram-scale products can be synthesized that contain almost exclusively nanofibers. The synthesis is based on the well-known chemical oxidative polymerization of aniline in a strongly acidic environment, with ammonium peroxydisulfate as the oxidant.<sup>21</sup> Instead of using the traditional homogeneous aqueous solution of aniline, acid, and oxidant, the polymerization is performed in an immiscible organic/aqueous biphasic system, to separate the byproducts (inorganic salts, oligomers, etc.) according to their solubility in the organic and aqueous phases. Films of the polyaniline nanofibers possess much faster gas phase doping/dedoping times compared with conventional cast films and therefore hold promise for sensor applications.

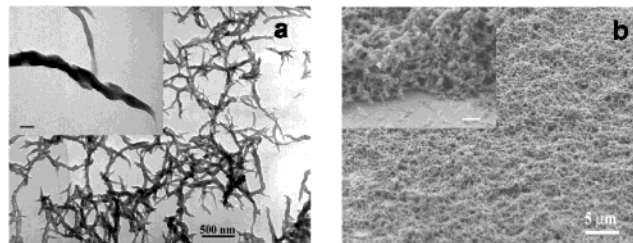


**Figure 1.** (a) TEM images of polyaniline/CSA nanofibers cast from a suspension after dialysis. The inset shows a twisted fiber (scale bar = 50 nm). (b) SEM secondary electron images of a thin film deposited on glass from the suspension. The inset shows a cross-sectional view of the film on the glass substrate (scale bar = 200 nm).

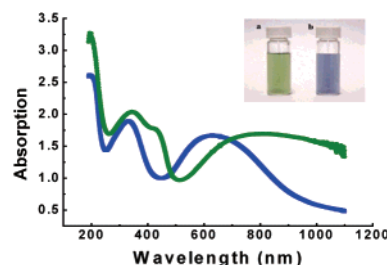


**Figure 2.** UV/vis spectra of polyaniline nanofibers after dialysis with water (green line + inset a), and with ammonium hydroxide (blue line + inset b).

In a typical synthesis, aniline is dissolved in an organic solvent, ( $\text{CCl}_4$ , benzene, toluene, or  $\text{CS}_2$ ), while ammonium peroxydisulfate is dissolved in water with camphorsulfonic acid (CSA). The two solutions are then carefully transferred to a beaker, generating an interface between the two layers. After 3–5 min, green polyaniline forms at the interface and then gradually diffuses into the aqueous phase. After 24 h, the entire water phase is filled homogeneously with dark-green polyaniline, while the organic layer appears red-orange, likely due to the formation of aniline oligomers. The aqueous phase is then collected, and the by-products are removed by dialysis against deionized water, using tubing with a ~12,000–14,000 MW cutoff (Fisher Scientific). When the deionized water bath reaches a pH of 7, 10  $\mu\text{L}$  of the suspension is diluted with 1 mL of deionized water for characterization with electron microscopy (Figure 1) and UV/vis spectroscopy (Figure 2). Dedoped polyaniline is obtained by dialysis using 0.1 M ammonium hydroxide and then deionized water. Synthetic yields range from 6 to 10 wt %.

Figure 1a shows a typical transmission electron microscopy (TEM, JEOL 100CX) image of the polyaniline/CSA complex made at the interface between water and  $\text{CCl}_4$  after dialysis. It is found in multiple TEM studies that >95% (volume fraction) of the sample are nanofibers with diameters of 30–50 nm. The lengths of the fibers range from 500 nm up to several micrometers. The nanofibers

<sup>†</sup> University of California.<sup>‡</sup> The Aerospace Corporation.

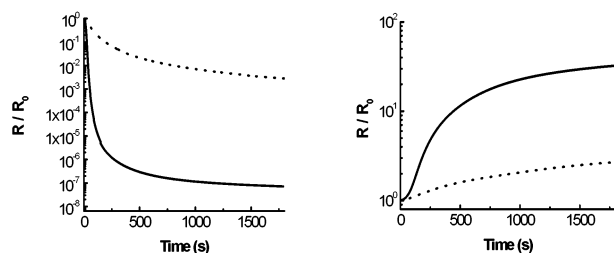


**Figure 3.** Resistance changes of a nanofiber emeraldine base thin film (solid line) and conventional (dotted line) film upon exposure to 100 ppm HCl vapor in nitrogen (left) and the same fully HCl doped films exposed to 100 ppm  $\text{NH}_3$  vapor in nitrogen (right).  $R/R_0$  is the resistance ( $R$ ) normalized to the initial resistance ( $R_0$ ) prior to gas exposure.

tend to agglomerate into interconnected nanofiber networks, rather than bundles.<sup>15</sup> A closer look at the nanofibers reveals that many of them are twisted, as shown in the inset to Figure 1a. The sample uniformity and narrow diameter distribution are also confirmed by field emission scanning electron microscopy (JEOL JSM-6401F) images. Figure 1b shows a typical SEM secondary electron image of a nanofiber thin film cast on a glass substrate from a dialyzed colloidal suspension. The sample appears to be exclusively nanofibers, consistent with the TEM images. Dedoping has no noticeable effect on the morphology of the fibers. All the other aqueous/organic systems including benzene, toluene, and  $\text{CS}_2$  produce similar polyaniline nanostructures.

Figure 2 presents the UV/vis (HP 8453) spectra of the doped (green line) and dedoped (blue line) nanofibers in water. The polyaniline/CSA complex forms a green suspension (inset a), after dialyzing against water, corresponding to doped polyaniline in its emeraldine salt form. Remarkably, these polyaniline/CSA nanofibers are stable in water in contrast to conventional polyaniline/CSA thin films, which can be dedoped by water. Since the polyaniline/CSA nanofibers have no absorption due to free CSA at  $\sim 285$  nm (Figure 2), CSA is most likely tightly incorporated as anions within the polyaniline backbone during the in situ polymerization of aniline in CSA solution. Dedoped polyaniline nanofibers (inset b) can be obtained by dialyzing the pristine polyaniline/CSA complex against 0.1 M ammonium hydroxide, which produces the emeraldine base form of polyaniline (Figure 2, blue line).

Once the CSA molecules are removed, these dedoped fibers respond to doping/dedoping significantly faster than conventionally undoped polyaniline. To examine the doping and dedoping of the nanofibers versus conventional films in more detail, a dedoped nanofiber emeraldine base thin film ( $\sim 2.5$   $\mu\text{m}$ ) and a conventional undoped thin film ( $\sim 1$   $\mu\text{m}$ ) were deposited on an array of interdigitated gold electrodes and exposed to HCl (doping) and then  $\text{NH}_3$  (dedoping). The array consists of 23 pairs of electrodes ( $4946$   $\mu\text{m} \times 40$   $\mu\text{m} \times 0.18$   $\mu\text{m}$ ) on a glass substrate, with gaps of  $40$   $\mu\text{m}$ .

Figure 3 shows the real-time resistance changes of dedoped films monitored with an electrometer (Keithley 617), upon exposure to 100 ppm of HCl (left), and the same fully HCl doped films exposed to 100 ppm of  $\text{NH}_3$  (right). The nanofiber thin film responds much

faster than the conventional film to both acid doping and base dedoping even though the nanofiber film is more than twice as thick. This is likely due to the small diameter of the nanofibers that gives rise to a high surface area within the film that can be accessed by the gas vapors. Surprisingly, the nanofiber films show essentially no thickness ( $0.2$ – $2.5$   $\mu\text{m}$ ) dependence in their performance. This is consistent with the porous nature of the nanofiber films, which enables gas molecules to diffuse in and out of the fibers rapidly. This also leads to a much greater extent of doping or dedoping over short times for the nanofiber films. Therefore, nanofiber films appear to have better performance in both sensitivity and time response compared to conventional films.

In summary, this aqueous/organic interfacial synthesis has the following advantages: (i) Both the synthesis and purification are simple with no template-removing steps needed. (ii) Uniform nanofibers comprising  $>95\%$  of each sample are readily produced. (iii) The synthesis is easily scalable and reproducible. Multiple syntheses performed from millimolar to molar quantities yield nanofibers of the same morphology, size distribution, and uniformity. (iv) The diameter of polyaniline fibers is at the nanoscale, which dictates their superior performance as chemical sensors. (v) The nanofibers are readily dispersed in water, which could facilitate environmentally friendly processing and biological applications.

**Acknowledgment.** We thank Dr. N. Presser (The Aerospace Corporation) for help with SEM images, the NSF for funding through an IGERT fellowship (S.V.), and The Aerospace Corporation for support (B.W., S.V.).

## References

- (1) Skotheim, T. A.; Elsenbaumer, R. L.; Reynolds, J. R. *Handbook of Conducting Polymers*, 2nd ed.; Marcel Dekker: New York, 1997.
- (2) Anderson, M. R.; Mattes, B. R.; Reiss, H.; Kaner, R. B. *Science* **1991**, 252, 1412–1415.
- (3) Cao, Y.; Smith, P.; Heeger, A. J. *Synth. Met.* **1993**, 57, 3514–3519.
- (4) Chiang, J. C.; MacDiarmid, A. G. *Synth. Met.* **1986**, 13, 193–205.
- (5) Xia, Y. N.; Wiesinger, J. M.; MacDiarmid, A. G.; Epstein, A. J. *Chem. Mater.* **1995**, 7, 443–445.
- (6) Majidi, M. R.; KaneMaguire, L. A. P.; Wallace, G. G. *Polymer* **1994**, 35, 3113–3115.
- (7) Wu, C. G.; Bein, T. *Science* **1994**, 264, 1757–1759.
- (8) Martin, C. R. *Chem. Mater.* **1996**, 8, 1739–1746.
- (9) Parthasarathy, R. V.; Martin, C. R. *Chem. Mater.* **1994**, 6, 1627–1632.
- (10) Wang, C. W.; Wang, Z.; Li, M. K.; Li, H. L. *Chem. Phys. Lett.* **2001**, 341, 431–434.
- (11) Michaelson, J. C.; McEvoy, A. J. *Chem. Commun.* **1994**, 79–80.
- (12) Qiu, H. J.; Wan, M. X. *J. Polym. Sci., Part A: Polym. Chem.* **2001**, 39, 3485–3497.
- (13) Wei, Z. X.; Zhang, Z. M.; Wan, M. X. *Langmuir* **2002**, 18, 917–921.
- (14) Yang, Y. S.; Wan, M. X. *J. Mater. Chem.* **2002**, 12, 897–901.
- (15) Huang, L. M.; Wang, Z. B.; Wang, H. T.; Cheng, X. L.; Mitra, A.; Yan, Y. X. *J. Mater. Chem.* **2002**, 12, 388–391.
- (16) Choi, S. J.; Park, S. M. *Adv. Mater.* **2000**, 12, 1547–1549.
- (17) Liu, J. M.; Yang, S. C. *Chem. Commun.* **1991**, 1529–1531.
- (18) Reneker, D. H.; Chun, I. *Nanotechnology* **1996**, 7, 216–223.
- (19) MacDiarmid, A. G.; Jones, W. E.; Norris, I. D.; Gao, J.; Johnson, A. T.; Pinto, N. J.; Hone, J.; Han, B.; Ko, F. K.; Okuzaki, H.; Llaguno, M. *Synth. Met.* **2001**, 119, 27–30.
- (20) He, H. X.; Li, C. Z.; Tao, N. J. *Appl. Phys. Lett.* **2001**, 78, 811–813.
- (21) Huang, W. S.; Humphrey, B. D.; MacDiarmid, A. G. *J. Chem. Soc., Faraday Trans.* **1986**, 82, 2385.
- (22) Yang, C. Y.; Cao, Y.; Smith, P.; Heeger, A. J. *Synth. Met.* **1993**, 53, 293–301.

JA028371Y